Structural Monitoring and Maintenance, *Vol. 6, No. 4 (2019) 365-387*
DOI: https://doi.org/10.12989/smm.2019.6.4.365

A parametric study on fatigue of a top-tensioned riser subjected to vortex-induced vibrations

Do Kyun Kim*[1,2], Eileen Wee Chin Wong[3a] and Mala Konda Reddy Lekkala[3b]

[1]Marine Offshore and Subsea Technology (MOST) Group, School of Engineering, Newcastle University, NE1 7RU Newcastle upon Tyne, UK
[2]Graduate Institute of Ferrous Technology, POSTECH, 37673 Pohang, Republic of Korea
[3]Ocean and Ship Technology Research Group (Department of Civil and Environmental Engineering), Universiti Teknologi PETRONAS, 32610 Seri Iskandar, Perak, Malaysia

(Received June 7, 2019, Revised August 6, 2019, Accepted August 15, 2019)

Abstract. This study aims to provide useful information on the fatigue assessment of a top-tensioned riser (TTR) subjected to vortex-induced vibration (VIV) by performing parametric study. The effects of principal design parameters, i.e., riser diameter, wall thickness, water depth (related to riser length), top tension, current velocity, and shear rate (or shear profile of current) are investigated. To prepare the base model of TTR for parametric studies, three (3) riser modelling techniques in the OrcaFlex were investigated and validated against a reference model by Knardahl (2012). The selected riser model was used to perform parametric studies to investigate the effects of design parameters on the VIV fatigue damage of TTR. From the obtained comparison results of VIV analysis, it was demonstrated that a model with a single line model ending at the lower flex joint (LFJ) and pinned connection with finite rotation stiffness to simulate the LFJ properties at the bottom end of the line model produced acceptable prediction. Moreover, it was suitable for VIV analysis purposes. Findings from parametric studies showed that VIV fatigue damage increased with increasing current velocity, riser outer diameter and water depth, and decreased with increasing shear rate and top tension of riser. With regard to the effects of wall thickness, it was not significant to VIV fatigue damage of TTR. The detailed outcomes were documented with parametric study results.

Keywords: vortex-induced vibration (VIV); fatigue; top-tensioned riser (TTR); parametric study; offshore

1. Introduction

The marine riser plays a recognized role as a bloodline, which is the principal component to transport the produced hydrocarbon from subsea wells to the offshore platforms and vice versa. This riser experiences vortex-induced vibration (VIV) caused by currents and this phenomenon may lead fatigue failures due to repeated cumulative fatigue damages. In this regard, the estimation of VIV fatigue damage is essential in designing a feasible and operable riser, especially for risers operating in deep water regions with severe environmental conditions. In the case of riser,

*Corresponding author, Senior Lecturer, Adjunct Professor, E-mail: do.kim@ncl.ac.uk
[a] MSc. Student
[b] Ph.D. Student

http://www.techno-press.org/?journal=smm&subpage=7 ISSN: 2288-6605 (Print), 2288-6613 (Online)

currents may be considered as the main loader that cause fatigue damage by VIV.

Understanding the influence of design parameters of TTR on the VIV fatigue damage of the riser is essential for efficient design process of the riser. Parametric or sensitivity studies are commonly performed to investigate the effects of each parameter. DNV (2010) advised users to perform sensitivity studies as great differences in the calculated fatigue damage results can be observed when the design parameters are varied. Sensitivity studies should be carried out for all possible parameters that may vary during the design life of the riser. Sensitivity studies can also be conducted to determine the factors that affect the fatigue damage results the most. By performing sensitivity studies, the effects of variation of design parameters on the VIV fatigue damage can be quantified by listed several parameters (Bai and Bai 2005). All these parameters may affect the accuracy of the estimation of fatigue damage of riser such as current profile, structural properties, frequency and magnitude of lift force, hydrodynamic damping and excitation and correlation length. Among all, current profile is the most significant parameter (Wong and Kim 2018). Design parameters that are related to riser geometry and loading applied to riser are the main interest when designing risers considering VIV fatigue. A number of studies have been conducted to analyse the effects of these parameters.

Wang (2008) analysed the effects of top tension, inner fluid density, current velocity profile, outer diameter, riser wall thickness, and elastic modulus on the VIV fatigue damage of deep-water risers. From his studies, top tension, outer diameter, elastic modulus, and current profile had a greater influence on fatigue damage than inner fluid density and wall thickness of riser. VIV fatigue damage may decrease with increasing top tension and lower elastic modulus of riser material. A larger outer diameter contributed to greater VIV fatigue damage. Effects of inner fluid density and riser wall thickness were less important as the variation of both parameters were limited. The relationship of the variation of riser outer diameter with VIV was consistent with the results from Zahari and Dol (2015) where the VIV amplitude of the cylinder increased with increasing cylinder diameter. Xu *et al.* (2017) also demonstrated a similar trend for the fatigue damage when the outer diameter of riser was increased. However, they discovered that the trend changes when the outer diameter of riser reached 0.6 m, at which they observed a decrease in fatigue damage when the outer diameter was 0.6 m due to decrease of vibration orders. The authors, however, did not provide the fatigue damage results for outer diameters greater than 0.6 m, hence it is unclear if the fatigue damage increases or decreases for risers with outer diameters beyond 0.6 m. The effects of current velocity and top tension on riser fatigue life were similar to the results by Wang (2008).

Roveri and Vandiver (2001) performed parametric studies on the SlenderEx system, which is a low-cost drilling system, using SHEAR7 to determine the effects of main parameters on the fatigue damage induced by VIV. Their study showed that an increase in bottom effective tension might contribute to a decrease in fatigue damage, whereas an increase in current velocities can lead to an increase in fatigue damage. The results of the influence of user-defined input parameters in SHEAR7 on the VIV fatigue damage of drilling riser in 1,900 m water depth by Roveri (2007) in later years agreed with results by Roveri and Vandiver (2001). Xue *et al.* (2014) used HanØtangen's riser model (Lie and Kaasen 2006) to conduct parametric studies. Similar to previous studies, risers with a higher top tension had higher natural frequencies, hence lower order modes may be excited which causes lower bending stress, cycle counting frequency, and lower fatigue damage. Sensitivity studies by Schiller *et al.* (2014) and Komachi *et al.* (2017) also showed that variation in top tension causes changes in excited modes. Vibration frequency increased with increasing top tension when the same mode was excited. Moreover, Xue *et al.* (2014) found that

fatigue damage of riser generally increased with internal fluid density. However, due to variation of excited modes, it was observed that the trend of fatigue damage was less regular and limited in certain ranges. Since their studies focused on the sheared current, it was found that fatigue damage was highly sensitive to top velocities in sheared current, as they observed a great increase in VIV fatigue damage when top velocity increased due to excitation of higher order nodes.

Schiller *et al.* (2014) studied the sensitivity of VIV of deep-water risers to current profile, shear and directionality. Their findings showed that uniform currents produced the largest response. Even with a large surface velocity in sheared currents, uniform currents with similar velocity still produced a larger response. The order of excited mode increased with the increasing uniform current velocity. In the sheared current, more modes were excited than in the uniform current. Number of excited modes increased with shear parameters. They deduced that velocity plays a more significant role in VIV response than intensity of the shear of currents. Xue *et al.* (2011) also suggested that strongly sheared currents excited more vibrating modes but did not always cause larger VIV fatigue damage. Fu *et al.* (2017) indicated that the effect of shear rates on the dominant vibration mode is less significant. General trends suggested that the dominant mode number increased with increasing shear rate, which may be caused by a larger maximum velocity in currents with a large shear rate. VIV is also very sensitive to riser lengths. Risers with longer lengths have a lower natural frequency, thus the velocity of current required to induce VIV is lower. Higher mode of vibration is induced in deep water risers than in shallow water risers. Higher modes have higher natural frequencies, hence the riser will have longer power-in regions which lead to greater VIV fatigue damages (Bai and Bai 2005, Xue *et al.* 2011, Low and Srinil 2016, Park *et al.* 2016). Luo *et al.* (2015) reported that longer cables have higher excitation frequencies and generally have more severe fatigue damage.

In the present study, the individual effect of each TTR design parameter was investigated. To prepare the base model of TTR for the parametric study, three riser-modelling techniques in OrcaFlex were investigated and validated against the reference model. The selected riser model was used to perform parametric studies to study the effect of design parameters on the VIV fatigue damage of TTR.

2. Modelling techniques of TTR

At the beginning of the analysis, TTR data was collected from several literatures to determine the suitable base model for a detailed VIV fatigue analysis. To perform a VIV analysis, the riser needs to be modelled. OrcaFlex which is well-known numerical code for offshore pipeline and riser engineers (Park *et al.* 2015, Ziwa *et al.* 2017), was selected to model the chosen TTR system from the literature. After the TTR was modelled, static analysis was carried out in OrcaFlex. Static analysis was performed to compute the global equilibrium configuration of the riser system upon the exertion of static loading such as weight, buoyancy of and hydrodynamic drag of the riser. The computed equilibrium configuration would be the starting position for VIV analysis. Upon completion of static analysis of TTR, VIV analysis of TTR was performed. The main aim when performing VIV analysis was to determine the VIV fatigue damage of the given riser configuration under the design current load. In this study, SHEAR7 was used to perform VIV analysis as it is commonly used by the industry for VIV prediction. A similar VIV analysis technique by adopting OrcaFlex and Shear7 software has been applied to steel catenary risers (Park *et al.* 2015, Kim *et al.* 2018, 2019).

To determine the best model for VIV analysis, three modelling approaches were developed and tested. To select the most appropriate modelling approach, the VIV fatigue results of each model were compared with the results of literature of the chosen TTR system. The models with a percentage difference of more than 10% were eliminated. The modelling approach that produces the lowest percentage difference of result with original literature result was selected. The selected TTR model was used for parametric studies to determine the effects of design parameters, which included riser outer diameter, wall thickness, top tension, water depth, current velocity and shear rate, on the VIV fatigue damage of TTR.

2.1 Riser model description

The base configuration without a strake riser system in the thesis by Knardahl (2012) was used as the reference model for the VIV analysis of the top tensioned riser. The riser is based on Aker Solution's workover riser system located northwest of Hammerfest in the Barents Sea. The water depth is 321 m.

Fig. 1 shows the riser stack-up configuration. The riser is modelled from diverter up to wellhead fixed to the seabed. The diverter is connected to the platform. A UFJ connecting telescopic joint to the diverter reduces the bending stresses and loads transmitters to the riser during platform motions. A telescopic joint, or also known as a slip joint, offsets the heave motion of the platform. Components following the telescopic joint are spacer joint and pup joint, which are shorter joints used to provide sufficient space-out.

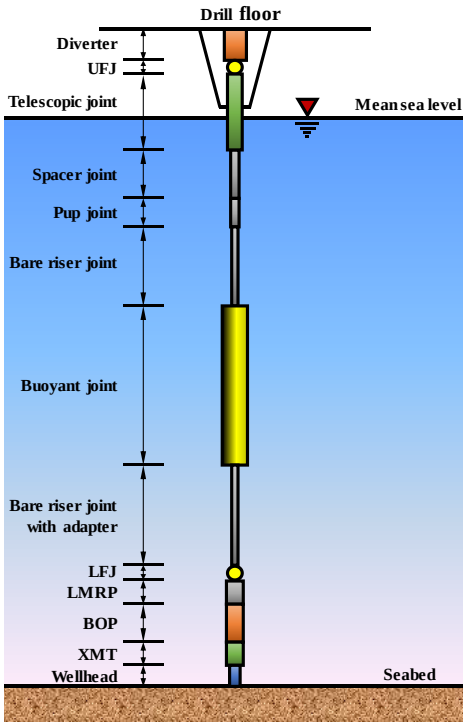

Fig. 1 Riser stack-up system

Table 1 Riser stack-up data (Knardahl 2012)

Component	Length (m)	Quantity	Outer diameter (m)	Buoyancy diameter (m)	Inner diameter (m)	Mass (kg)
Diverter	6.18	1	1.575	-	1.511	3410
UFJ	1.525	1	0.612	-	0.495	5210
Telescopic joint	31.24	1	0.660	-	0.483	40131
Spacer joint	12.87	1	0.556	-	0.495	10520
Pup joint	7.63	1	0.556	-	0.495	6230
Bare riser	22.86	2	0.533	-	0.495	13910
Riser with buoyancy module	22.86	7	0.533	1.397	0.495	13910
Bare riser with adapter	23.86	3	0.533	-	0.495	13910
LFJ	1.525	1	0.612	-	0.495	5210
LMRP	3.0	1	0.737	-	0.476	85409
BOP	9.0	1	0.737	-	0.476	194591
XMT	2.4	1	0.737	-	0.476	55000
Wellhead	3.2	1	1.000	-	0.452	60000

Following the pup joint is riser joint, with approximately 50% of the riser joint covered with buoyance modules to reduce the required top tension. Adapters at the bottom end of the riser provide crossover from the riser joint to lower flex joint (LFJ). LFJ connects the lower end of the riser joint to the lower marine riser package (LMRP) and reduces the bending force acting on the LMRP. LMRP is fixed to the blowout preventer (BOP) which in turn is fixed to the Christmas Tree (XMT). The whole riser stack-up is fixed to the wellhead. Table 1 shows the geometry properties and masses of the components of the riser stack-up. Steel is used as the material of the riser, with a density of 7,860 kg/m^3 and Young's modulus of 210 GPa. The bending stiffness, axial stiffness and torsional stiffness for each component are presented in Table 2.

The platform is assumed to be still at mean position of 0 for VIV analysis; hence drift-off is neglected. Since VIV analysis using SHEAR7 solely considers current load without considering wave-induced VIV, wave load and wind load is assumed to be zero (0). The current profile used for VIV fatigue analysis is presented in Fig. 2. The current heading direction is assumed to be 0 degree. TTR has same configuration in all directions, hence a single direction current load is assumed to be sufficient. The current direction along the water depth is assumed to be unidirectional. There is no change in the current heading direction along the water column.

Single slope S-N curve is adopted for fatigue damage calculation. F2 S-N curve for submerged structures in seawater is used in case stress concentration factor is not applied. The detail of the S-N curve is presented in Table 3, where 'a' is intercept on cycle axis for S-N curve and b is the slope of the S-N curve (Knardahl 2012).

Table 2 Bending, axial and torsional stiffness of line component (Knardahl 2012)

Component	Bending stiffness ($\times 10^6$) (kNm2)	Axial stiffness ($\times 10^6$) (kN)	Torsional stiffness ($\times 10^6$) (kNm2)
Diverter	9.791	32.885	7.572
UFJ	0.001140	21.40	100.00
Telescopic joint	1.408	33.686	1.089
Spacer joint	0.369721	10.675	285.94
Pup joint	0.369721	10.675	285.94
Bare riser	0.215096	6.504	166.35
Riser with buoyancy module	0.215096	6.504	166.35
Bare riser with adaptor	0.215096	6.504	166.35
LFJ	0.004020	21.40	100.00
LMRP	2.510	89.59	100.00
BOP	2.510	89.59	100.00
XMT	2.510	89.59	100.00
Wellhead	9.880	164.9	100.00

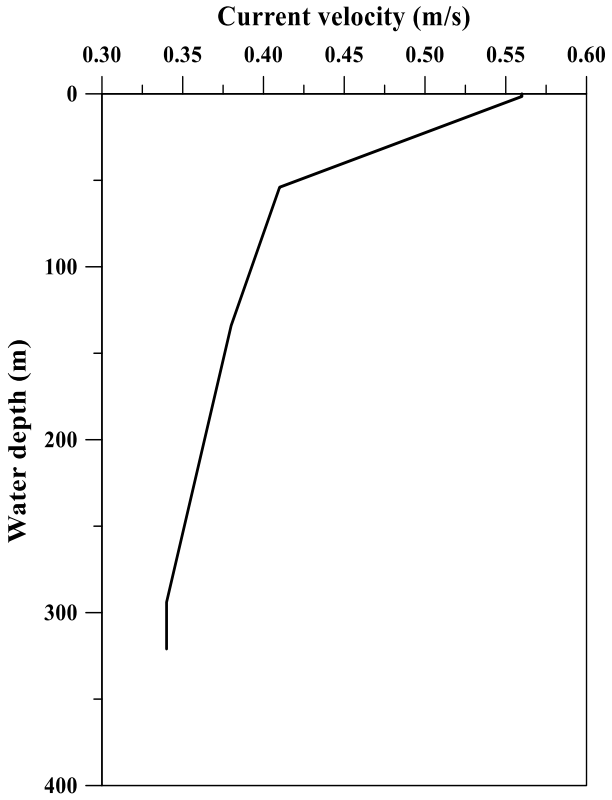

Fig. 2 Current profile

Table 3 S-N curve parameters (Knardahl 2012)

S-N curve	F2
Intercept (a)	11.63
Slope of curve (b)	3

2.2 Boundary condition and modelling assumption

In OrcaFlex, the riser was modelled in line with the lumped mass (Orcina 2012). This study primarily investigated the VIV fatigue damage of the riser caused by current loads. Several assumptions and simplifications were made on the riser model to give prominence to the VIV fatigue due to current load. Listed below are the assumptions made throughout the study. The modelling of the riser is limited to 2D, with the influence of platform motion to the fatigue damage of riser being neglected. Hence, the platform is assumed to be still as suggested by Bai and Bai (2005). Concurring with above preceding assumption, the wave load and wind load effects are omitted to solely analyze current-contributed VIV (Bai and Bai 2005). The wave-induced VIV is not investigated in this study.

The flow rate of internal fluid is not considered in the study to eliminate the effects of slugging and flow of internal fluid in the riser. The telescopic joint can be modelled as a pipe in a pipe model to account for the relative motion between the inner barrel and outer barrel of the telescopic joint due to heave motion from the platform. However, the heave motion of the platform is not considered in this study as mentioned in the scope of study. Therefore, it is acceptable to model the telescopic joint as a single pipe. Since the riser is modelled as a simple cylinder in OrcaFlex, the diameters of the auxiliary lines (kill and choke lines) are included in the equivalent outer and inner diameter of the main riser pipe.

The masses of auxiliary lines and operational fluids in the auxiliary lines are counted in the total mass of the riser joint. The bending and axial stiffness of the riser pipes are calculated as the multiple of moments of inertia of the riser pipe cross-section and the Young's modulus of steel. The stiffness of the auxiliary lines is deemed to be small and negligible (ISO 2009).

The focus of this study is the VIV fatigue of the riser pipe. In the following modelling method sub-section, the lower stack of the system including the LMRP, BOP, XMT and wellhead is either omitted or modelled as a circular cylinder with equivalent cross-section that simulates the bending and axial stiffness of the lower stack (ISO 2009). Soil-structure interaction is not considered in this context. For the detailed pipe or riser and soil interaction matters, following research outcomes may be referred (Yu *et al.* 2013, 2015, 2017, Kim *et al.* 2017). Linear soil response modelled as a constant linear stiffness is adopted in the model, which is current industry practice (Quéau 2015).

In compliance with the assumptions, the riser model is designed as a fixed-free condition. The bottom end of the riser model is set to be fixed at the seabed in all translation and rotation. The top end of the riser model is set to be free to move in the vertical direction. The tension force of 5,500kN is applied as an axial force at the top end of riser. The tension force is determined based on the effective weight of the riser with approximately 400kN effective tension at the end of the riser (Knardahl 2012).

2.3 Modelling approaches

Literature has presented multiple ways of modelling the top tensioned riser in OrcaFlex, each with different aims and focus of study. Unlike SCR, TTR consists of stack-up of different components. Depending on the problem of study and the available input data, the modelling of each section along riser differs. In some literature, the riser model ends at the LFJ with pinned condition while others model the complete riser stack-up up until the wellhead is fixed on the seabed (Vafin 2015, Xu *et al.* 2017). In fact, ISO (2009) suggests several modelling approaches to conform with various concerns and accessible model data. To determine the suitable model for VIV analysis, three modelling methods were studied and validated against the VIV response results from Knardahl (2012).

2.3.1 Model 1

In the first approach, the riser is modelled until the LFJ. The bottom boundary conditions of the riser in this model is different from the other two approaches. The bottom end of the riser is pinned at the connection to lower stack. The top end of the riser provided constant tension force. A similar simplification is used by Cunff *et al.* (2002) and Xu *et al.* (2017). Fig. 3 illustrates Model 1 which was created in OrcaFlex. Tension is applied at the top end of the riser as a constant point load since the tension system data and stroke-out information is not provided. A single line model is used to construct the riser in the OrcaFlex. The line starts with the diverter and ends with the LFJ. Diverter, telescopic joint, spacer joint, pup joint, bare riser, riser with buoyancy module and bare riser with adapters are modelled as homogeneous pipes, as they are assumed to made from single homogeneous material. UFJ and LFJ are modelled as general lines since axial and bending stiffness can be inputted directly. The bottom end of the LFJ is set to be pinned connection with rotation stiffness of 46 kNm/deg (Knardahl 2012).

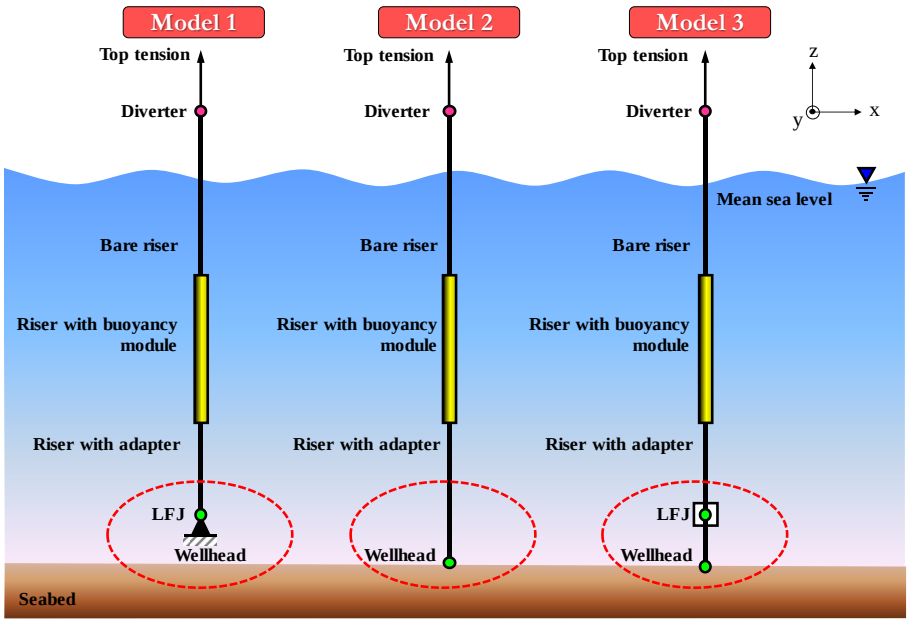

Fig. 3 Assumed top-tensioned riser models in OrcaFlex

2.3.2 Model 2

For the second model, riser is modelled until the wellhead, as portrayed in Fig. 3. The bottom end of the model is fixed on the seabed in all directions. All the components in the riser stack-up are modelled as a single line model, which is the same approach used by Jang (2016). LMRP, BOP, XMT and wellhead are included in the line model and modelled as a general line with bending and axial stiffness inputted directly. These lower stacks are represented as circular cylinders with cross-sections that provide equivalent stiffness and mass. Like the previous model, top tension is modelled as a single point load. In this model, lower stacks are also included in the VIV analysis. As the result, the stiffness and diameter of the lower stacks will also influence the fatigue damage distribution along the riser pipe.

2.3.3 Model 3

Model 3 follows the drilling riser example provided by the OrcaFlex software. A similar modelling approach is also adopted by Vafin (2015). Model 3 uses a two-line model connected with a 6D buoy. The first line model consists of a diverter, UFJ, telescopic joint, spacer joint, pup joint, riser joint, buoyant joint and LFJ. Modelling of the first line is the same as Model I. Top tension is applied at the end of diverter as point load. The lower end of LFJ is connected to the 6D Buoy with negligible properties. The 6D buoy functions as a connection point with six degrees of freedom for first and second lines. The translation and moment are transmitted from the first line to the second line through the 6D buoy. The top end of the second line connects to the 6D buoy with infinity rotational stiffness, as the lower stacks are large and have very high stiffness. The second line model is composed of LMRP, BOP, XMT and wellhead, which are modelled as general line. The bottom end of the wellhead is fixed to the seabed in all directions. Fig. 3 shows the riser model 3 in OrcaFlex.

3. Selection of modelling technique

All three models presented were previously designed with the same current load applied to all three models. After completing the models, static analysis was performed in OrcaFlex to calculate the initial configuration of riser at equilibrium under the weights, buoyancy and current loads. Modal analysis was carried out to determine the natural frequency of the riser, which was then used by SHEAR7 to analyse the VIV response of the riser. The process was iterated until the static position of the riser converged. Fatigue damage was then computed from the VIV response. VIV analysis results were presented and compared with the results from Knardahl (2012). This paper focuses on the VIV response of riser pipes up to LFJ, whereas Knardahl investigated the VIV response of the whole riser stack-up. Hence, only the VIV response of the section from diverter to LFJ of the riser stack-up in Knardahl's paper was used to compare with the results of the three models.

The maximum fatigue damage of risers starting from the diverter to the LFJ in Models 1, 2, 3 and Knardahl's model are presented in Table 4. The percentage of differences of the fatigue damage between Model 1, 2, 3 and Knardahl's model are listed in the last column of Table 4. Fatigue damage of riser in Model 3 showed the lowest percentage difference (2.962%) from Knardahl's model, followed by Model 1. Model 2 showed a very high fatigue damage in risers compared to other three models. Hence, the modelling approach for Model 2 was not appropriate in this application.

Table 4 VIV amplitude and percentage difference of models

Model	Maximum fatigue damage (1/yr)	Percentage difference (%)
Model 1	8.709×10^{-3}	3.13
Model 2	8.030	94,990.01
Model 3	8.695×10^{-3}	2.96
Knardahl (2012)	8.445×10^{-3}	-

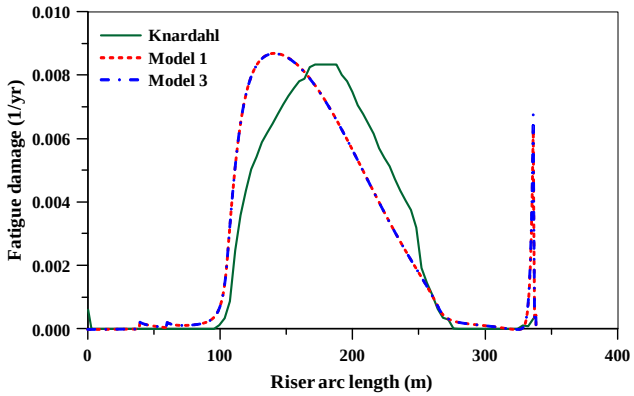

Fig. 4 Comparison of fatigue damage distribution along the riser between models

Fig. 4 shows the comparison of fatigue damage distribution along the riser for Model 1, 3 and Knardahl's model. A similar trend of fatigue damages was observed by above three models (1, 3 and Knardahl's). The fatigue damage peaked at the buoyant joint and increased again near the end of LFJ. All three models had maximum fatigue damage at the buoyant joint. The location of the maximum peaks of the fatigue damage of Model 1 and 3 were offset from Knardahl's model, but the maximum value of the fatigue damage is close. At the end of LFJ, fatigue damage in Model 1 and 3 increased much higher than in Knardahl's model. The deviation of the result may be caused by different calculation methods applied by SHEAR7 used for Model 1 and 3 compared to calculation methods applied by VIVANA software used in Knardahl's model.

Judging from the comparison results of mode frequency, VIV amplitude and fatigue damage of three developed models with Knardahl's model, both Model 1 and Model 3 produced results that were similar to Knardahl's results. Between the two, Model 3 had the smallest difference in results from Knardahl's model. In terms of simulation time, Model 1 required less computational time than Model 3 because Model 1 contained only a single line model whereas Model 3 contained a two-line model and one buoy model which required more time to calculate the equilibrium position. Considering the time required to generate all the simulation results for the parametric study, Model 1 is deemed to be the most appropriate model for further study. Furthermore, the result difference between Model 1 and Model 3 was insignificant. For these reasons, Model 1 was selected as the final model for subsequent study. To conclude, the modelling approach in Model 1 was validated against Knardahl's model and thus it is suitable for VIV analysis purposes.

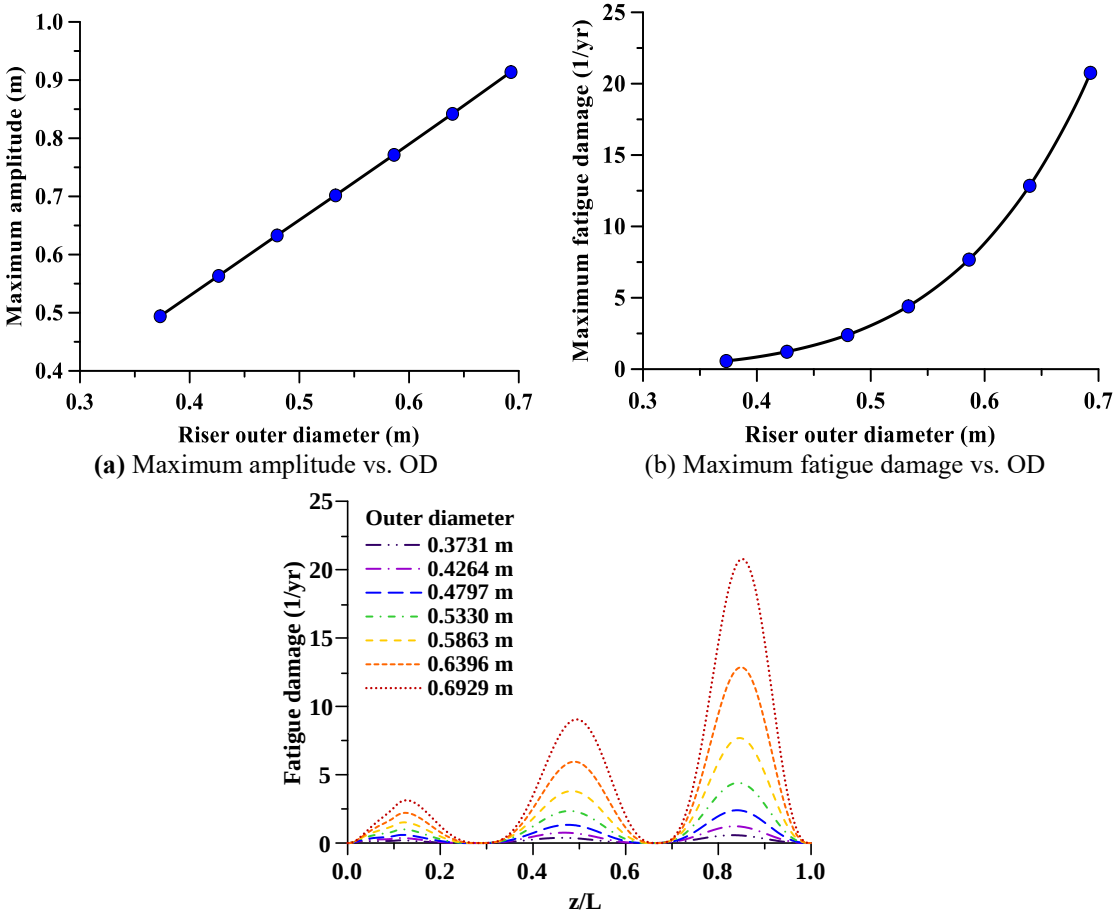

(a) Maximum amplitude vs. OD

(b) Maximum fatigue damage vs. OD

(c) Fatigue damage vs. z/L

Fig. 5 Result comparison between risers of different outer diameters

4. Fatigue design considerations by parametric studies

Parametric studies were performed on the TTR model to understand the significance of each design parameter in affecting the VIV fatigue damage of riser. To study the individual effects of the variation in the outer diameter and wall thickness of the riser pipe, the base riser configuration was simplified to a single bare riser as to eliminate other possible factors or interactions affecting the results comparison. Current profile in the base model was set to a uniform current of 0.7 m/s to concentrate on the individual effects of current velocity and shear profile. The design parameters investigated were geometrical properties of the riser, tension and current profile properties.

4.1 Effect of riser outer diameter

The effect of the outer diameter was studied by varying the outer diameter of the riser with a

10%, 20% and 30% increase and decrease from the base case. In the base case, the riser had an outer diameter of 0.533 m. 7 cases were formed. In all cases, the risers had same wall thickness of 19 mm. A constant top tension of 5,500 kN was applied at the top end of the risers. The maximum fatigue damage results are compared by considering the effect of outer diameter changes in Table 5. For all cases, it is observed that a single mode is excited and mode 3 is the dominant excited mode. Fig. 5(a) shows that an increase in the outer diameter of riser increases the maximum vibration amplitude, which is consistent with results by Zahari and Dol (2015). As the result, the maximum VIV fatigue damage of the riser increases with the outer diameter, as shown in Figs. 5(b) and 5(c), which agrees with results discovered by Wang (2008) and Xu *et al.* (2017).

4.2 Effects of riser wall thickness

Six (6) parametric cases were constructed by 10%, 20% and 30% increase and decrease from base case, as listed in Table 6. In all cases, the risers had the same dimension and constant top tension. Maximum VIV fatigue damage of each pipe of different wall thickness is shown in Table 6 and the percentage difference between each case and base case were computed. Mode 3 is excited for all cases of wall thickness. The maximum fatigue damage of the riser decreases as the wall thickness increases and then, it increases with the wall thickness as illustrated in Fig. 6(a).

Table 5 Comparison results of TTR with varying outer diameters

Case	Riser outer diameter (m)	Parameter difference	Dominant mode No.	Dominant mode frequency (Hz)	Maximum fatigue damage (1/yr)	Percentage difference (Compared to Base case)
1	0.3731	-30%	3	0.249	0.579	-86.9%
2	0.4264	-20%	3	0.249	1.229	-72.1%
3	0.4797	-10%	3	0.249	2.399	-45.6%
Base	0.5330	0	3	0.249	4.407	–
4	0.5863	10%	3	0.249	7.684	74.4%
5	0.6396	20%	3	0.249	12.856	191.7%
6	0.6929	30%	3	0.249	20.771	371.3%

Table 6 Comparison result of TTR with varying riser wall thickness

Case	Riser wall thickness (m)	Parameter difference	Dominant mode No.	Dominant mode frequency (Hz)	Maximum fatigue damage (1/yr)	Percentage difference (Compared to Base case)
1	0.0133	-30%	3	0.249	4.4941	2.0%
2	0.0152	-20%	3	0.249	4.4425	0.8%
3	0.0171	-10%	3	0.249	4.4140	0.2%
Base	0.0190	0	3	0.249	4.4072	–
4	0.0209	10%	3	0.249	4.4205	0.3%
5	0.0228	20%	3	0.249	4.4538	1.1%
6	0.0247	30%	3	0.249	4.5074	2.3%

Table 7 Comparison result of TTR with varying water depth

Case	Water depth (m)	Parameter difference	Dominant mode No.	Dominant mode frequency (Hz)	Maximum fatigue damage (1/yr)	Percentage difference (Compared to Base case)
1	192.6	-40%	2	0.268	4.2717	-3.1%
2	224.7	-30%	2	0.230	1.6807	-61.9%
3	256.8	-20%	2	0.201	0.7452	-83.1%
4	288.9	-10%	3	0.284	8.2858	88.0%
Base	321.0	0	3	0.254	4.4072	–
5	353.1	10%	3	0.228	2.4923	-43.4%
6	385.2	20%	3	0.208	2.2821	-48.2%
7	417.3	30%	4	0.262	8.0378	82.4%
8	449.4	40%	4	0.239	5.2659	19.5%

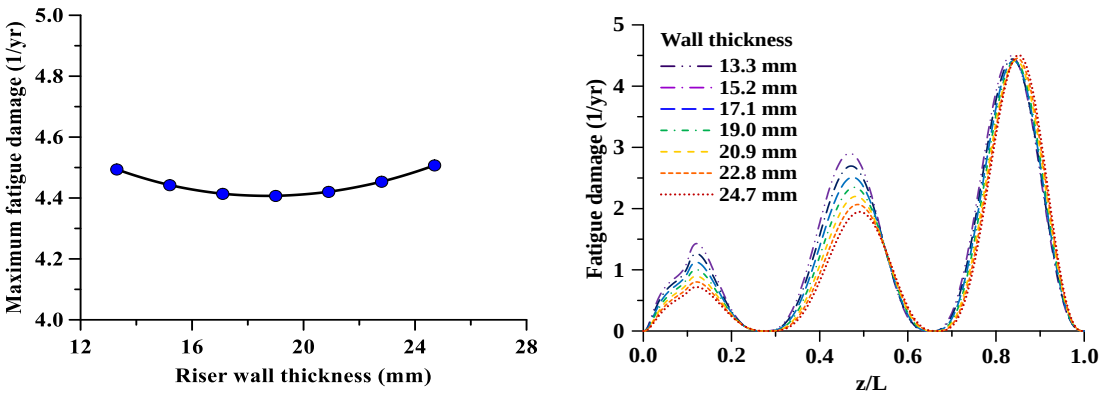

(a) Maximum fatigue damage vs. wall thickness (b) Fatigue damage vs. z/L

Fig. 6 Result comparison between risers of different wall thickness

However, Fig. 6(b) shows that fatigue damage increases with wall thickness along the risers, except at the last peak where fatigue damage is nearly equal in all cases. The increase of fatigue damage with increase in wall thickness from thickness of 0.019 m to 0.0247 m is consistent with findings by Li *et al.* (2010), but not for the case of 1 to 3. Table 6 shows that the percentage difference between each case is small, less than 3% in all cases. This indicates the effect of wall thickness is less significant, as agreed by Wang (2008).

4.3 Effect of water depth

The effect of water depth on VIV fatigue damage of the riser was studied by varying the water depth while keeping other parameters fixed. Risers had the same outer diameter of 0.533 m, wall thickness of 19 mm and constant top tension of 5,500 kN at the top end of the risers. Eight

parametric cases were constructed with a 10%, 20%, 30% and 40% increase and decrease from the base case, as listed in Table 7. Extra two (2) more cases were added to investigate the effect of water depth compared to other effects, in order to study the trends at the boundary.

Table 7 and Fig. 7(b) show that there are three (3) kinds of different dominant excited modes. It is found that mode 2 is dominant in cases 1 to 3, mode 3 dominates in cases 4 to 6, whereas mode 4 dominates in case 7 and 8. As water depth increases, the length of riser required increases. Longer risers have lower natural frequencies as portrayed in Fig. 7(a), which is consistent to observations made by Xue *et al.* (2011).

Since current velocities and outer diameters of risers are constant in all cases, the Strouhal frequency is 0.227 for all cases. With lower natural frequencies and constant Strouhal frequencies as riser length increases, a higher mode is excited. The result is consistent with statement by Bai and Bai (2005).

The dominant excited mode frequency decreases as water depth increases but jumps when there is a shift in the dominant mode as illustrated in Fig. 7(b). A similar trend is observed in fatigue damage changes with water depths in Fig. 7(c). After considering all assumed scenarios, maximum fatigue damage increases as water depth increases because a higher mode is excited, similar to results presented by Luo *et al.* (2015). Fig. 7(d) shows the distribution of fatigue damage along the risers in all cases. A significant percentage difference between case 4 and the base case suggests the importance of variation of water depth in contributing to changes in VIV fatigue damage.

4.4 Effect of top tension

The top tension applied at top end of riser varied from 2,750 kN to 6,050 kN for risers with outer diameters of 0.533 m and wall thickness of 19 mm. Fig. 8(a) shows that maximum vibration amplitude decreases until the top tension is 3,850 kN. When tension exceeds 3,850 kN, the maximum amplitude abrupt jumps to a peak at a tension of 4,400 kN and decreases gradually with top tension. The reason behind the discontinuation in the maximum amplitude graph is the change in the dominant excited mode. Like the observation made by Schiller *et al.* (2014) and Komachi *et al.* (2017), the natural frequency of the riser varies when the top tension of riser is changed. Likewise, the mode that is excited by the constant vortex shedding frequency varies depending on the top tension. For case 1 to 3, the dominant mode is mode 4.

When the top tension is 4,400 kN or higher than this, the dominant mode shifts to lower mode 3 as demonstrated in Table 8. Fig. 8(c) shows that the maximum fatigue damage of the riser decreases as the top tension increases with a sudden downtrend after 3,850 kN. Upon exceeding 4,400 kN, the maximum fatigue damage decreases slowly. The discontinuation is also caused by a shift of the dominant excited mode to the lower mode, which can be observed from the shift in the fatigue damage distribution in Fig. 8(d).

As the top tension increases, a lower mode number is excited, leading to a lower maximum RMS stress as seen in Fig. 8(b). These results agree with those by Wang (2008), Roveri and Vandiver (2001) and Li *et al.* (2010). The percentage difference of the fatigue damage between each case with the base case in Table 8 is large when the dominant mode No. changes. This shows that the influence of top tension to VIV response of riser is significant and the top tension should be carefully designed.

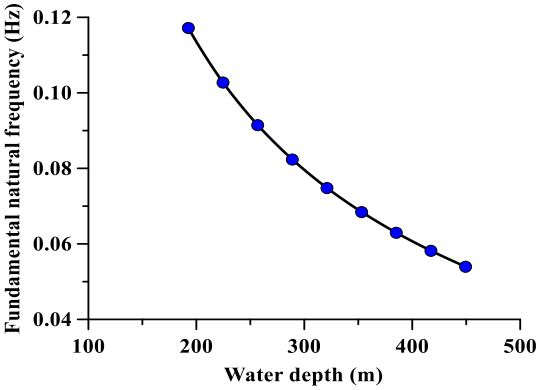

(a) Fundamental natural frequency vs. depth

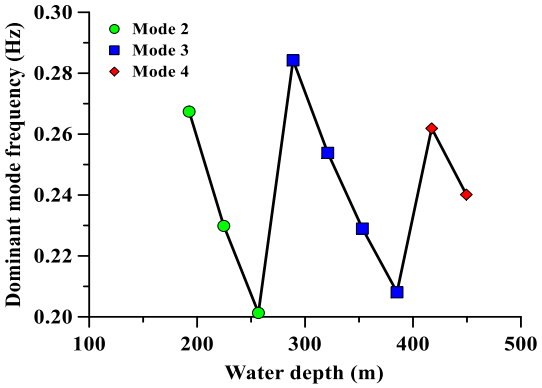

(b) Dominant mode frequency vs. water depth

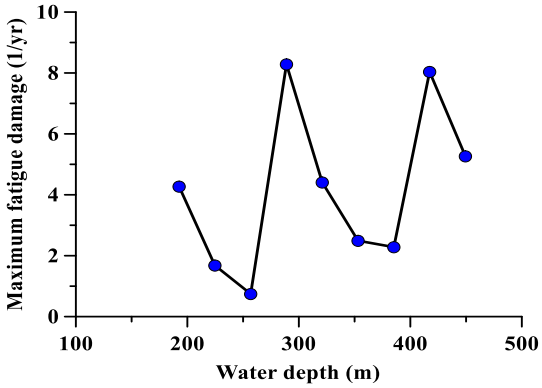

(c) Maximum fatigue damage vs. water depth

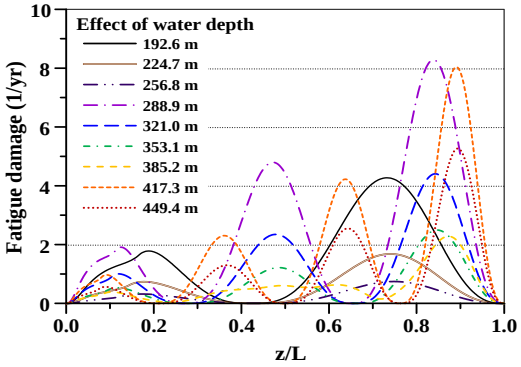

(d) Fatigue damage vs. z/L

Fig. 7 Results comparison between cases of different water depths

Table 8 Comparison result of TTR with varying riser top tension

Case	Riser top tension (kN)	Parameter difference	Dominant mode No.	Dominant mode frequency (Hz)	Maximum fatigue damage (1/yr)	Percentage difference (Compared to Base case)
1	2,750	-50%	4	0.262	52.7460	1096.8%
2	3,300	-40%	4	0.262	44.4940	909.6%
3	3,850	-30%	4	0.262	29.3280	565.5%
4	4,400	-20%	3	0.254	4.5060	2.2%
5	4,950	-10%	3	0.254	4.4332	0.6%
Base	5,500	0	3	0.254	4.4072	–
6	6,050	10%	3	0.254	4.4042	-0.1%

Table 9 Comparison result of TTR with varying current velocities

Case	Current velocity (m/s)	Parameter difference	Dominant mode No.	Dominant mode frequency (Hz)	Maximum fatigue damage (1/yr)	Percentage difference (Compared to Base case)
1	0.49	-30%	2	0.160	0.1833	-95.8%
2	0.56	-20%	2	0.160	0.1880	-95.7%
3	0.63	-10%	3	0.254	4.2737	-3.0%
Base	0.70	0	3	0.254	4.4072	–
4	0.77	10%	3	0.254	4.5082	2.3%
5	0.84	20%	3	0.254	4.5864	4.1%
6	0.91	30%	4	0.351	40.2430	813.1%

4.5 Effect of current velocity

To study the effect of the current velocities, six (6) cases with different uniform current velocities of 10%, 20% and 30% increase and decrease from the base case were constructed respectively, as shown in Table 9. In all cases, the risers had same dimension, length and constant top tension. The current profile applied on the riser was uniform. Table 9 shows that different dominant vibration modes were excited under different current velocities. The dominant excited mode increased as the current velocity increased, as depicted in Fig. 9(a). From Figs. 9(b)-9(c), it is observed that maximum VIV fatigue damage of riser increases with the increasing current velocity. The fatigue damage along the risers in Fig. 9(c) also shows the change in the distribution shape when there is a shift in the dominant excited mode. As presented by Schiller *et al.* (2014), higher modes are excited in higher current velocity conditions, leading to a greater modal curvature and greater fatigue damage.

This result is consistent with previous studies done by Wang (2008) and Xu *et al.* (2017). The large percentage differences between the cases indicate the significant influence of current velocity on the VIV response of riser.

4.6 Effect of shear rate

To study the effect of shear profiles of currents, six cases with different linearly sheared current profiles were created by varying the shear rate, ΔS from 0 to 0.003s^{-1} with interval of 0.0005s^{-1}. The current profile was defined using the equation provided by Schiller *et al.* (2014). It was formulated in such the way that all the linearly sheared profiles shared the same kinetic energy as the original uniform current with velocity of 0.7 m/s.

$$u(z) = u_0 \frac{2u_0 - \Delta S z}{\left(4u_0^2 - 2u_0 \Delta S L + \frac{1}{3}\Delta S^2 L^2\right)^{0.5}} \tag{1}$$

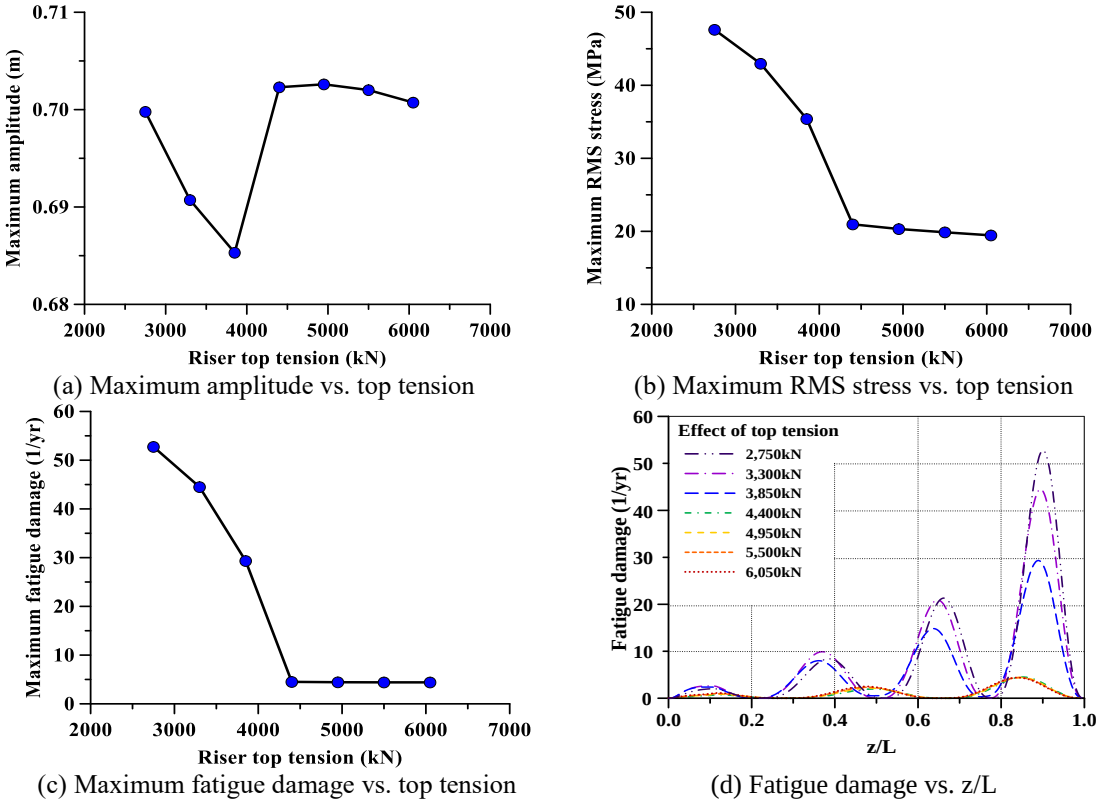

(a) Maximum amplitude vs. top tension

(b) Maximum RMS stress vs. top tension

(c) Maximum fatigue damage vs. top tension

(d) Fatigue damage vs. z/L

Fig. 8 Result comparison between TTR with different top tension

Table 10 Comparison result of TTR with varying shear rates

Case	Shear rate (s^{-1})	Dominant mode No.	Dominant mode frequency (Hz)	Maximum fatigue damage (1/yr)	Percentage difference (Compared to Base case)
Base	0	1	0.079	4.4072	–
1	0.0005	1	0.079	4.4435	0.8%
2	0.0010	1	0.079	4.4853	1.8%
3	0.0015	2	0.160	3.6800	-16.5%
4	0.0020	3	0.254	2.1069	-52.2%
5	0.0025	3	0.254	1.0435	-76.3%
6	0.0030	3	0.254	1.0299	-76.6%

where u is the current velocity along the water column and u_0 is the corresponding uniform current velocity. The calculated current profiles are shown in Fig. 10. In all cases, the risers had the same dimension, length and constant top tension as in Section 4.5.

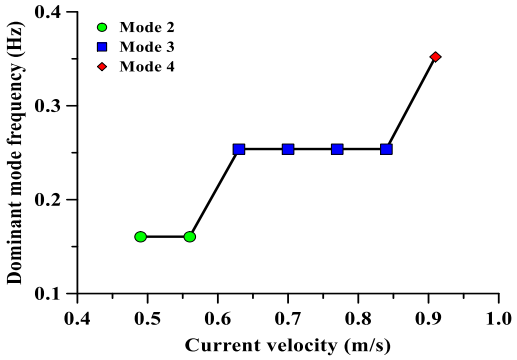

(a) Dominant mode frequency vs. current velocity

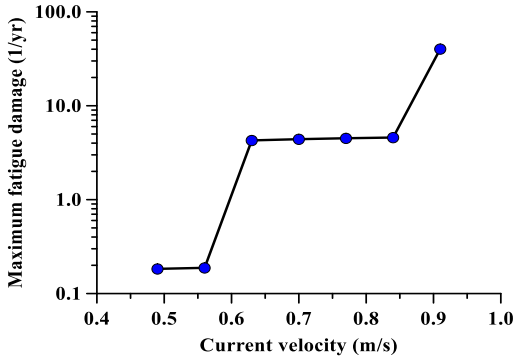

(b) Maximum fatigue damage vs. current velocity

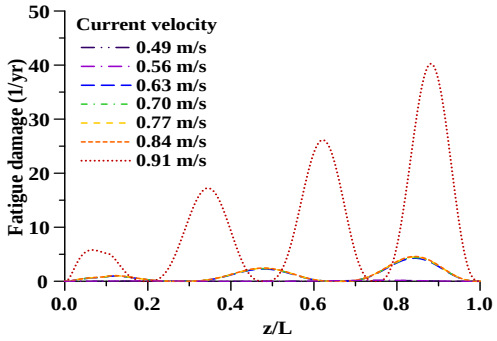

(c) Fatigue damage vs. z/L

Fig. 9 Result comparison between TTR under different current velocities

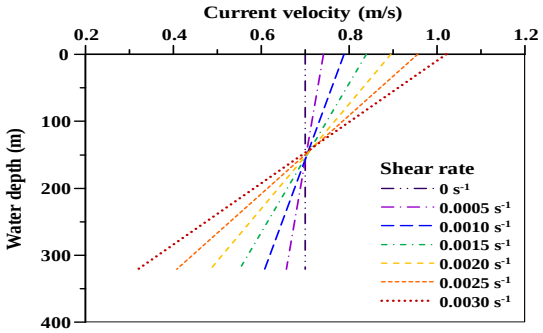

Fig. 10 Linearly sheared current profile

Same dominant vibration mode, mode No. 3, is excited under different current profiles. Table 10 shows that as the shear rate increases, the number of excited mode increases. This is consistent with observation provided by Schiller *et al.* (2014). In Fig. 11(a), it is observed that the maximum amplitude of the riser first increases slightly with the shear rate until $0.001s^{-1}$ and then decreases greatly with the increasing shear rate. The increasing trend of the amplitude at the beginning is

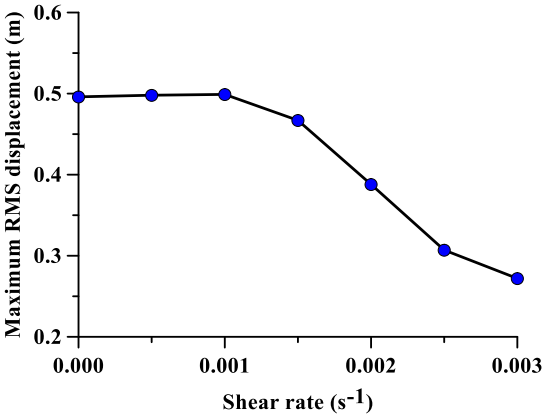

(a) Maximum RMS displacement vs. shear rate

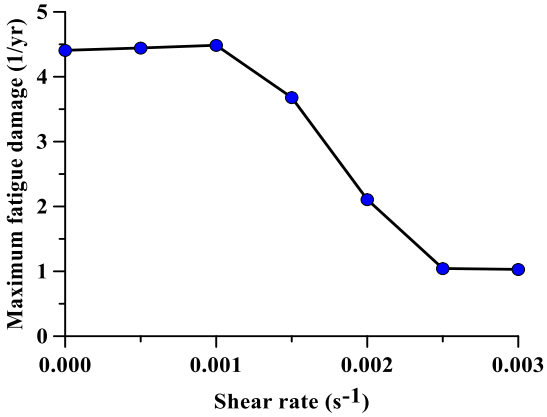

(b) Maximum fatigue damage vs. shear rate

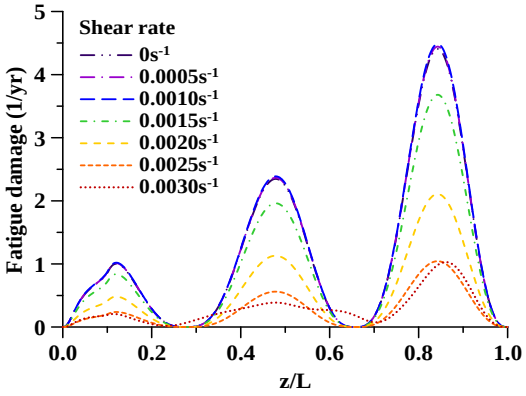

(c) Fatigue damage vs. z/L

Fig. 11 Result comparison between TTR under different sheared current profile

slightly different from the inference. reported by Schiller *et al.* (2014). The plausible reason behind the difference in result is the number of excited modes.

In the first three cases, only one mode is excited. Hence, it can be inferred that VIV fatigue damage depends on the number of excited modes along the risers. The fatigue damage along the risers in Figs. 11(b) and 11(c) also shows similar trend as the maximum amplitude graph. The higher the shear rate, the higher modes excites.

Thus, there is a lower maximum VIV fatigue damage in the riser because the fatigue damage is more distributed along the risers. The percentage difference between the cases are high as represented in Table 10 indicating the significance of shear rate in VIV fatigue damage prediction. Variation in current velocities has a greater effect on VIV fatigue damage of riser than shear rate, as proven by the higher percentage difference between cases with varying current velocities. This observation agrees with the findings by Schiller *et al.* (2014).

5. Conclusions

Parametric studies were performed to investigate the effects of design parameters on VIV fatigue damage of TTR. Based on the obtained results, the following conclusions were drawn.

- 30% increase in the outer diameter of TTR contributed to a 371.3% increase in maximum VIV fatigue damage.
- Fatigue damage increased by 2.3% with a 30% increase in wall thickness. Hence, the difference between different cases of wall thickness was insignificant.
- Deeper water depth required a longer riser length with lower natural frequencies. Maximum VIV fatigue damage generally increased by 82.4% with a 30% increase in water depth due to a higher excitation mode.
- The higher the top tension of TTR, lower mode number was excited; hence, TTR had lower maximum RMS stress and lower maximum VIV fatigue damage. A 30% decrease in top tension lead to about 500% increase in top tension.
- The maximum VIV fatigue damage increased nearly 800% with a 30% increase in current velocity due to higher mode numbers being excited.
- The higher the shear rate of the current profile, more modes of the TTR were being excited, causing the fatigue damage to be more spread out along the riser, hence causing lower maximum VIV fatigue damage.

Overall, riser outer diameter, water depth, top tension and current profile in term of velocity and shear rate had great influence on the VIV fatigue damage of TTR. On the other hand, the effect of wall thickness of riser was less significant. The results of the parametric studies formed the basis for design consideration during the riser design process.

For future studies, a simplified VIV assessment method can be developed using the defined function relating each parameter to maximum fatigue damage of riser. It is observed that the identification of the excited mode is significant to calculate the VIV fatigue damage of riser, hence it shall be incorporated in the VIV calculation. Continuous validation and improvement shall be done to enhance the accuracy and precision of the VIV calculation approach.

Acknowledgements

This research was supported by the Technology Innovation Program (Grant No.: 10053121 and 10051279) funded by the Ministry of Trade, Industry & Energy (MI, Korea) and YUTP Grant (015LC0-096, Malaysia). The authors would also like to thank for the great support of POSTECH, Republic of Korea.

References

Bai, Y. and Bai, Q. (2005), *Subsea Pipelines and Risers*, Elsevier Ltd., Oxford. UK.

DNV (2010), *Riser Fatigue* (RP-F204), Det Norske Veritas, Oslo, Norway.

Fu, B., Zou, L. and Wan, D. (2017), "Numerical study on the effect of current profiles on vortex-induced vibrations in a top-tension riser", *J. Mar. Sci. Appl.*, **16**(4), 473-479. https://doi.org/10.1007/s11804-017-1429-3.

ISO (2009), *Petroleum and Natural Gas Industries - Drilling and Production Equipment* (ISO 13624-1), International Organization for Standardization, Geneva, Switzerland.

Jang, M.W. (2016), "Drilling riser system analysis for ultra-deepwater", MSc. Dissertation, Graduate School of Engineering Mastership, Pohang University of Science and Technology (POSTECH), Pohang, Korea.

Knardahl, G.M. (2012), "Vortex induced vibrations of marine risers", MSc. Dissertation, University of Science and Technology (NTNU), Trondheim, Norwegian.

Komachi, Y., Mazaheri, S. and Tabeshpour, M. (2017), "The effect of shifting natural frequency on the reduction of vortex-induced vibrations of marine risers", *Int. J. Coastal Offshore Eng.*, **1**(1), 9-16. https://doi.org/10.18869/acadpub.ijcoe.11.9.

Kim, D.K., Incecik, A., Choi, H.S., Wong, E.W.C., Yu, S.Y. and Park, K.S. (2018), "A simplified method to predict fatigue damage of offshore riser subjected to vortex-induced vibration by adopting current index concept", *Ocean Eng.*, **157**, 401-411. https://doi.org/10.1016/j.oceaneng.2018.03.042.

Kim, D.K., Wong, E.W.C., Lee, E.B., Yu, S.Y. and Kim, Y.T. (2019), "A method for the empirical formulation of current profile", *Ships Offshore Struct.*, **14**(2), 176-192. https://doi.org/10.1080 /17445302.2018.1488340.

Kim, Y.T., Kim, D.K., Choi, H.S., Yu, S.Y. and Park, K.S. (2017), "Fatigue performance of deepwater steel catenary riser considering nonlinear soil effect", *Struct. Eng. Mech.*, **61**(6), 737-746. https://doi.org/10.12989/sem.2017.61.6.737.

Le Cunff, C., Biolley, F., Fontaine, E., Etienne, S. and Facchinetti, M.L. (2002), "Vortex-induced vibrations of risers: theoretical, numerical and experimental investigation", *Oil & Gas Sci. Technol.*, **57**(1), 59-69. https://doi.org/10.2516/ogst:2002004.

Li, X., Guo, H. and Meng, F. (2010), "Fatigue life assessment of top tensioned risers under vortex-induced vibrations", *J. Ocean Univ. China*, **9**(1), 43-47. https://doi.org/10.1007/s11802-010-0043-7.

Lie, H. and Kaasen, K.E. (2006), "Modal analysis of measurements from a large-scale VIV model test of a riser in linearly sheared flow", *J. Fluids Struct.*, **22**(4), 557-575. https://doi.org /10.1016/j.jfluidstructs.2006.01.002.

Low, Y.M. and Srinil, N. (2016), "VIV fatigue reliability analysis of marine risers with uncertainties in the wake oscillator model", *Eng. Struct.*, **106**, 96-108. https://doi.org/10.1016/j.engstruct. 2015.10.004.

Luoa, G., Chen, J. and Zhou, X. (2015), "Effects of various factors on the VIV-induced fatigue damage in the cable of submerged floating tunnel", *Polish Maritime Res.*, **22**(4). https://doi.org /76-83. 10.1515/pomr-2015-0075.

Orcina (2012), "*OrcaFlex User's Manual* (Version 9.6a)", Daltongate, UK.

Quéau, L.M. (2015), "Estimating the fatigue damage of steel catenary risers in the touchdown zone", Ph.D. Dissertation, University of Western Australia, Crawley, Australia.

Park, K.S. Kim, Y.T., Kim, D.K., Yu, S.Y. and Choi, H.S. (2015). "Structural analysis of deepwater steel catenary riser using OrcaFlex", *J. Ocean Eng. Technol.*, **29**(1), 16-27. https://doi.org/10.5574/KSOE.2015.29.1.016.

Park, K.S., Kim, Y.T., Kim, D.K., Yu, S.Y. and Choi, H.S. (2016), "A new method for strake configuration of Steel Catenary Risers", *Ships Offshore Struct.*, **11**(4), 385-404. https://doi.org/10.1080/17445302.2014.999479.

Roveri, F.E. (2007), "A sensitivity study on fatigue damage of a drilling riser caused by vortex-induced vibrations", *Proceedings of the 39th Offshore Technology Conference* (OTC 2007), Houston, USA (OTC-19026). https://doi.org/10.4043/19026-MS.

Roveri, F.E. and Vandiver, J.K. (2001), "Slenderex: using shear7 for assessment of fatigue damage caused by current induced vibrations", *Proceedings of the 20th International Conference on Offshore Mechanics and Arctic Engineering* (OMAE 2001), Rio de Janeiro, Brazil (OMAE01-1163).

Schiller, R.V., Caire, M., Nóbrega, P.H.A., Passano, E. and Lie, H. (2014), "Vortex induced vibrations of deep water risers: sensitivity to current profile, shear and directionality", *Proceedings of the 33rd International Conference on Ocean, Offshore and Arctic Engineering*, San Francisco, USA (OMAE2014-24141). https://doi.org/10.1115/OMAE2014-24141.

Vafin, A. (2015), "Simulation-based assessment of drilling riser and its application for the Kara Sea region",

MSc. Dissertation, University of Stavanger, Stavanger, Norway.
Wang, Y.F. (2008), "Prediction methods for the VIV-induced fatigue damage in deep sea risers", PhD. Dissertation, Shanghai Jiaotong University, Shanghai, China.
Wong, E.W.C. and Kim, D.K. (2018), "A simplified method to predict fatigue damage of TTR subjected to short-term VIV using Artificial Neural Network", *Adv. Eng. Softw.*, **126**, 100-109. https://doi.org/10.1016/j.advengsoft.2018.09.011.
Xu, J., Wang, D., Huang, H., Duan, M., Gu, J. and An, C. (2017), "A vortex-induced vibration model for the fatigue analysis of a marine drilling riser", *Ships Offshore Struct.*, **12**(S1), 280-287. https://doi.org/10.1080/17445302.2016.1271557.
Xue, H., Guo, J., Tang, W. and Zhang, S. (2011), "Characteristic analysis of VIV-induced fatigue damage of top tensioned risers based on simplified model", *J. Offshore Mech. Arctic Eng.*, **133**(2), 0213041-1-7. https://doi.org/10.1115/1.4002046.
Xue, H., Tang, W. and Qu, X. (2014), "Prediction and analysis of fatigue damage due to cross-flow and in-line VIV for marine risers in non-uniform current", *Ocean Eng.*, **83**(1), 52-62. https://doi.org/10.1016/j.oceaneng.2014.03.023.
Yu, S.Y., Choi, H.S., Lee, S.K., Do, C.H. and Kim, D.K. (2013), "An optimum design of on-bottom stability of offshore pipelines on soft clay", *Int. J. Naval Architect. Ocean Eng.*, **5**(4), 598-613. https://doi.org/10.2478/IJNAOE-2013-0156.
Yu, S.Y., Choi, H.S., Lee, S.K., Park, K.S. and Kim, D.K. (2015), "Nonlinear soil parameter effects on dynamic embedment of offshore pipeline on soft clay", *Struct. Eng. Mech.*, **53**(5), 881-896. https://doi.org/10.1515/ijnaoe-2015-0016.
Yu, S.Y., Choi, H.S., Park, K.S., Kim, Y.T. and Kim, D.K. (2017), "Advanced procedure for estimation of pipeline embedment on soft clay seabed", *Struct. Eng. Mech.*, **62**(4), 381-389. http://doi.org/10.12989/sem.2017.62.4.381.
Zahari, M. and Dol, S. (2015), "Effects of different sizes of cylinder diameter on vortex-induced vibration for energy generation", *J. Appl. Sci.*, **15**(5), 783-791. http://dx.doi.org/10.3923/jas.2015. 783.791.
Ziwa, M.Z., Kim, D.K., Mustaffa, Z. and Choi, H.S. (2017), "A systematic approach to pipe-in-pipe installation analysis", *Ocean Eng.*, **142**, 478-490. https://doi.org/10.1016/j.oceaneng.2017.07.004.

JK

Abbreviations

BOP = Blowout preventer
DNV= DET NORSKE VERITAS
ISO = International Organization for Standardization
LFJ = Lower flex joint
LMRP = Lower marine riser package
SCR = Steel catenary riser
TTR = Top tensioned riser
UFJ = Upper flex joint
VIV = Vortex-induced vibration
XMT= Christmas tree